Software Demonstrator to Study Room Temperature Influence on Microvascular Blood Flow

A. Humeau-Heurtier [*] **G. Mahé** [**] **R. Guyonneau** [*]
P. Abraham [***]

[*] *Univ Angers, LARIS - Laboratoire Angevin de Recherche en Ingénierie des Systèmes, 62 avenue Notre-Dame du Lac, 49000 Angers, France (e-mail: {anne.humeau,remy.guyonneau}@univ-angers.fr).*
[**] *Univ Rennes 1, University hospital of Rennes, Pôle imagerie médicale et explorations fonctionnelles, Inserm CIC 1414, Hôpital Pontchaillou, 35033 Rennes Cedex 9, France (e-mail: guillaume.mahe@chu-rennes.fr)*
[***] *Univ Angers, University hospital of Angers, Laboratoire de Physiologie et d'Explorations Vasculaires, UMR CNRS 6214-INSERM 1083, 49033 Angers cedex 01, France (e-mail: piabraham@chu-angers.fr)*

Abstract: Skin microcirculation plays an essential role in human thermoregulation. The ambient temperature (room temperature) is one of the parameters that influences skin temperature, and thus skin microcirculation. The goal of our software demonstrator is to study, with a recent image processing algorithm, the variations of microvascular perfusion induced by variations of room temperatures. For this purpose, laser speckle contrast imaging (LSCI) data recorded in the forearm of 15 healthy subjects, in two room temperatures (17.2 ± 1.5°C and 31.4 ± 0.7°C), are processed. Three physiological states are studied: rest, biological zero, and post-occlusive reactive hyperaemia (PORH). The data are processed with the multi-dimensional complete ensemble empirical mode decomposition with adaptive noise (MCEEMDAN) algorithm. MCEEMDAN leads to intrinsic mode functions (IMFs) and a residue that reflect features of the original data and local textures with characteristic spatial frequencies. These features are not visible on raw LSCI perfusion images. Our results show that the features extracted by MCEEMDAN vary with the physiological state. Moreover, we reveal that the room temperature has an impact on the patterns extracted by MCEEMDAN, specially at PORH. MCEEMDAN results therefore probably reflect the microvessels state (vasoconstriction or vasodilation). However, these modifications induced by the room temperature in the patterns are different for IMFs and residue. They therefore vary with the spatial scales extracted by MCEEMDAN. Our demonstrator thus confirms the necessity to monitor the room temperature during microvascular studies. It also brings new research directions to improve the knowledge of temperature regulation of microvascular flow.

Keywords: Image processing, data-driven algorithm, empirical mode decomposition, biomedical, microcirculation, skin, temperature.

1. INTRODUCTION

Skin plays an important role in the body thermoregulation. This is performed through vasodilation and vasoconstriction of the skin vessels (microcirculation). Body cooling produces cutaneous vasoconstriction through a generalized increase of adrenergic vasoconstrictor activity. Body warming induces vasodilation through the decrease of spontaneous vasoconstrictor activity and partially via an active vasodilation mechanism (Charkoudian (2003)). Several factors can modify skin temperature, such as fever, exercise, environmental temperature variations...

Through this software demonstrator our goal is to study, with a recent image processing algorithm, the variations of microvascular perfusion induced by variations of room temperatures. More precisely, through an image processing algorithm, we herein extract local patterns from bidimensional microvascular perfusion data, and analyze how these patterns evolve with room temperatures. The monitoring of microvascular perfusion can be performed with several techniques. The probably most well known is laser Doppler flowmetry (LDF) (Nilsson et al. (1980a,b); Nilsson (1984); Humeau et al. (2007)). LDF has the advantage of giving real-time perfusion data but has the drawback of being a single-point technique. Recently, laser speckle contrast imaging (LSCI) has been proposed as an alternative technique to monitor microvascular perfusion.

LSCI is a wide-field imaging modality to measure blood flow in superficial tissues, such as skin (Briers and Webster (1996); Boas and Dunn (2010); Briers et al. (2013); Humeau-Heurtier et al. (2013)). The technique consists in illuminating the tissue under study with a coherent light. The resulting random interference patterns are captured by a camera. Due to the movements of the dynamic scatterers in the tissue, the interference patterns (speckle patterns) appear blurry. The amount of blur is related to the speed of the scatterers. The degree of blurring is quantified by the speckle contrast K computed as $K(x,y) = \frac{\sigma_N}{\mu_N}$ where σ_N and μ_N are respectively the standard deviation and mean of the pixel intensity in a neighborhood N around the pixel $P(x,y)$. The microvascular perfusion is inversely proportional to the contrast K. LSCI has the advantage of being contactless and gives bidimensional perfusion data (images) that have high temporal and spatial resolutions. Moreover, the instrument can be made with low cost devices and the measures are reproducible (Roustit et al. (2010a); Puissant et al. (2013); Richards et al. (2013); Humeau-Heurtier et al. (2014)).

In our work, LSCI data were acquired in healthy subjects, at different room temperatures. After acquisitions, we processed LSCI data in order to study how microvascular perfusion evolves. Our objective was also to analyze local patterns of LSCI data for each room temperature.

2. MATERIALS AND METHODS

2.1 Acquisition procedure

Fifteen healthy volunteers participated in this study which was approved by the local ethics committee of our university hospital (CPP-Ouest II, Angers, France). All participants provided written, informed consent prior to participation and the work was carried out in accordance with the Declaration of Helsinki. During the experiments, the participants rested in the supine position, and all the tests were performed in a quiet room after an acclimatization period of 20 min. For each subject, microvascular perfusion on the right forearm was monitored with a laser speckle contrast imager (PeriCam PSI System, Perimed), having a laser wavelength of 785 nm. The imager gives perfusion in laser speckle perfusion units (LSPU). The acquisition frequency of the images was 16 Hz. The distance between the laser head and skin surface was fixed at around 15 cm, which gave images with a resolution around 0.4 mm. Local cutaneous temperature was also measured on the right forearm using a surface thermocouple probe connected to an electronic thermometer (BAT-12, Physitemp Instruments Inc.).

Recordings were performed in two different room temperatures: 17.2 $\pm$ 1.5°C and 31.4 $\pm$ 0.7°C (Araham et al. (2013)). A minimal interval of one day separated each experiment and the order of studied temperatures was randomized.

The monitoring of microvascular blood flow was performed at rest, but also during a 3-minute period of occlusion (biological zero, BZ; cuff inflation to 50 mmHg above the systolic pressure), and during post-occlusive reactive hyperaemia (PORH). For each subject and for each room temperature, three images (19 $\times$ 19 pixels) have been processed: one at rest, one during the BZ, and one during PORH.

2.2 Image processing procedure

The interpretation of LSCI data is often difficult and an average of the perfusion in a region of interest (ROI) is often performed by the clinicians (Rousseau et al. (2011); Humeau-Heurtier et al. (2015a); Ansari et al. (2016)). This leads to a loss of the bidimensional approach of the perfusion. In order to overcome this problem, the multi-dimensional complete ensemble empirical mode decomposition with adaptive noise (MCEEMDAN) algorithm has recently been proposed (Humeau-Heurtier et al. (2015b)).

MCEEMDAN is a fully data-adaptive method that decomposes multi-dimensional data (as images) into components: several intrinsic mode functions (IMFs) and a residue. This decomposition reveals local textures with characteristic spatial frequencies (Humeau-Heurtier et al. (2015b)). The first IMF represents the finest textural (the background noise), while the last one gives only the largest scale of the overall mean trend in intensity of the image. From an algorithm point of view, the original image (matrix) is considered as a collection of one-dimensional series in the two directions (x and y). Each one-dimensional series is decomposed with the improved CEEMDAN algorithm described in Colominas et al. (2014). In the 2D case, the MCEEMDAN algorithm is therefore the following (Humeau-Heurtier et al. (2015b))

(1) decompose each row of the image (in ascending order) using the improved CEEMDAN algorithm. This leads to the first stage IMFs
(2) reconstruct the corresponding IMFs into two-dimensional data as the decomposition results in the first stage
(3) use improved CEEMDAN to decompose the results of step (ii) iteratively along the column in ascending order. This leads to the second-stage IMFs
(4) reconstruct the corresponding IMFs of the second stage into two-dimensional data as the decomposition results in the second stage
(5) the final IMFs are obtained by combining the IMFs that have comparable minimal scales

For n-dimensional data, the decomposition starts with the first dimension, and proceeds to the second and third, until all the dimensions are exhausted. When applied to LSCI data, MCEEMDAN is able to reveal hidden patterns that differ with physiological states (Humeau-Heurtier et al. (2015b)).

In the present work, two IMFs (IMF1 and IMF2) and the residue have been computed for each image (i.e. for the $3 \times 15 = 45$ images). Moreover, in order to quantify the results, the lacunarity of the fractal dimension image for each IMF and residue has been determined. Lacunarity

is a fractal property that is used to describe the texture of a fractal. More precisely, the fractal dimension of a structure provides a measure of its texture complexity. The higher the lacunarity, the more inhomogeneous the examined fractal area and vice versa. Lacunarity is defined in terms of the ratio of the variance over the mean value of the function as

$$L = \frac{1/(MN)\sum_{m=0}^{M-1}\sum_{n=0}^{N-1} I(m,n)^2}{\left[1/(MN)\sum_{k=0}^{M-1}\sum_{l=0}^{N-1} I(k,l)\right]^2} - 1, \qquad (1)$$

where M and N are the sizes of the fractal dimension image I (Petrou (2006)). In our work, fractal dimension has been computed using the differential box counting algorithm (Humeau-Heurtier et al. (2015b)).

3. RESULTS

The local cutaneous temperatures obtained by the low and high room temperatures were 28.0 ± 2.0°C and 34.1 ± 1.3°C, respectively. Moreover, the mean perfusion values for the 15 subjects, during the three states (rest, BZ, and PORH) were the following: 30.1 LSPU, 11.7 LSPU, 75.3 LSPU, respectively, for the low room temperature; 41.1 LSPU, 11.2 LSPU, and 98.6 LSPU, respectively, for the high room temperature.

The IMFs and residue extracted by MCEEMDAN are presented in Figs. 1 to 3. From these figures we observe patterns (hidden in raw LSCI data). The latter are visible at rest, and mostly during PORH; less during the BZ. Furthermore, at rest and at PORH, these patterns are much more visible at the high room temperature than at the low room temperature.

The lacunarity values for each room temperature and for each IMF/residue are shown in Figs. 4 and 5. We note that the lacunarity values computed at rest, during the BZ, and at PORH are close to each other for the low room temperature, for IMF1 and IMF2. More differences are observed for the high room temperature.

From Figs. 4 and 5 we also observe that, for the finest textural (IMF1 and IMF2), low room temperature reduces the lacunarity value at rest and at PORH, compared to the high skin temperature. By opposition, for the largest spatial scales (residue), at PORH, the lacunarity value is the highest for the lowest room temperature.

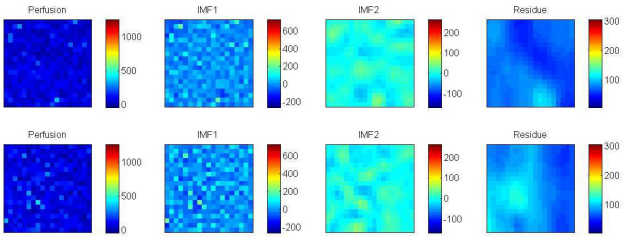

Fig. 1. MCEEMDAN results at rest for the low (upper panels) and high (lower panels) room temperature.

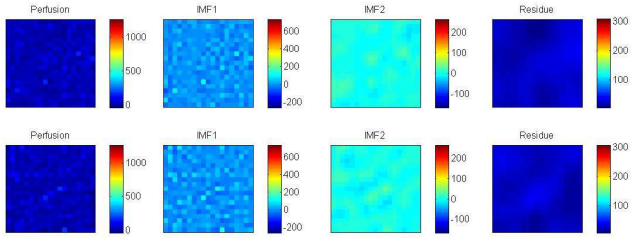

Fig. 2. MCEEMDAN results during the biological zero for the low (upper panels) and high (lower panels) room temperature.

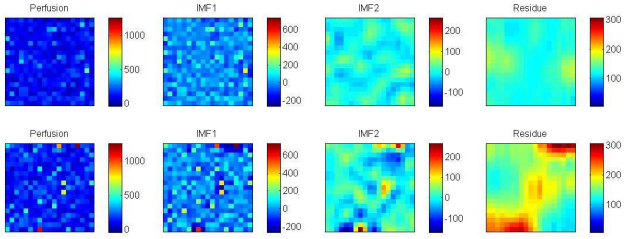

Fig. 3. MCEEMDAN results at PORH for the low (upper panels) and high (lower panels) room temperature.

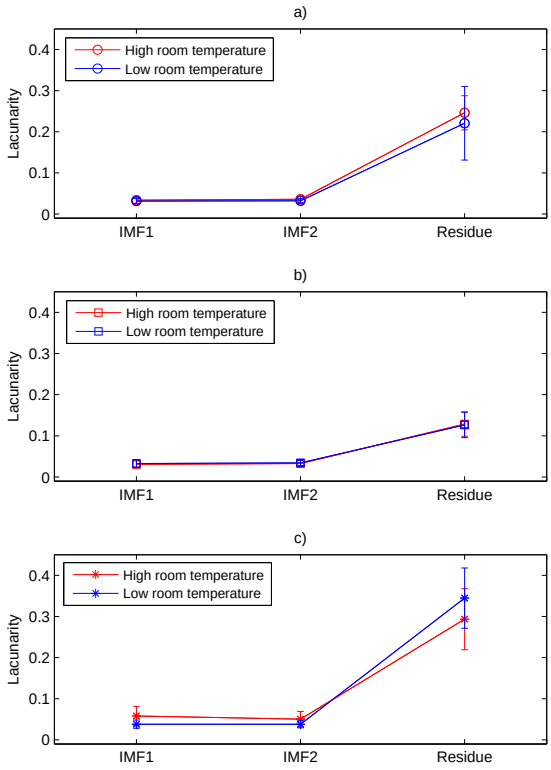

Fig. 4. Lacunarity (average and standard deviations computed from 15 subjects) of fractal dimension images for (a) Rest; (b) BZ; (c) PORH, given by MCEEMDAN.

4. DISCUSSION

The goal of our software demonstrator was to study, with a recent image processing algorithm, the variations

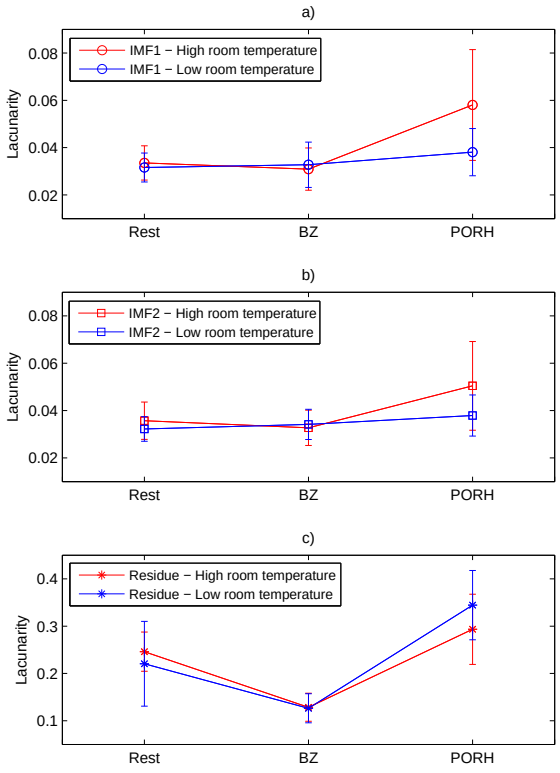

Fig. 5. Lacunarity (average and standard deviations computed from 15 subjects) of fractal dimension images for (a) IMF1; (b) IMF2; (c) residue, given by MCEEMDAN.

of microvascular perfusion induced by variations of room temperatures. For this purpose, LSCI data were recorded in 15 subjects, at two room temperatures. Skin temperature was also monitored during the experiments. The mean skin temperatures observed for the 15 subjects show that the room temperatures chosen lead to variations in cutaneous temperatures.

Our work shows that the patterns extracted by MCEEMDAN are influenced by the physiological state (rest, BZ, PORH) but also by the room temperature, specially at PORH. Furthermore, we reveal that the influence of the room temperature is different for IMFs and residue. Our findings therefore confirm the necessity to monitor the room temperature during microvascular investigations.

In the MCEEMDAN algorithm, IMFs can be considered as features of the original data and reveal local textures with characteristic spatial frequencies. The first IMF may represent the background noise and as the number of IMF increases, perfusion at different spatial scales are captured. From a clinical point of view, our results are interesting for three main reasons: first, our study reveals underlying patterns that are not visible on perfusion data. These patterns change with the physiological state (rest, BZ, PORH). During BZ, blood flow in the microcirculation is reduced, whereas it increases during PORH. Therefore, the patterns, that correspond to a *physical* signature on IMF1, IMF2, and residue, could also correspond to a *physiological* signature (microvascular signature). Second, the patterns revealed by MCEEMDAN also change with the room temperature. In the general cases, at high room temperatures we have a skin vasodilation state, while a more vasoconstricted state is obtained for lower room temperatures. The modification of the patterns with the room temperature therefore supports the idea that the patterns revealed by MCEEMDAN could reveal a *physiological* signature. Moreover, MCEEMDAN could also become an interesting tool to obtain a *bi-dimensional map* of the microvascular *reactivity* to ambient temperature. This leads to much more information than a perfusion *average* performed in a ROI. Third, our results show that, for the finest textural (IMF1 and IMF2), low skin temperature reduces the lacunarity value at rest and at PORH, compared to the high skin temperature. By opposition, for the largest spatial scales (residue), at PORH, the lacunarity value is the highest for the lowest skin temperature. Therefore, our work reveals that the microvascular modifications brought by variations of the room temperature depend on the spatial scales. This brings new research directions to improve the knowledge of temperature regulation of microvascular flow. The physiological phenomena coming into consideration to explain that, for IMF1 and IMF2, low skin temperature reduces the lacunarity value at rest and at PORH, compared to the high skin temperature, but that for the largest spatial scales (residue), at PORH, the lacunarity value is the highest for the lowest skin temperature, remain to be clarified. It has already been shown that room temperature plays a role on raw perfusion data (Araham et al. (2013)). Our results show that the modifications of microvascular perfusion generated by different room temperatures are also visible on IMFs and residue. However, these modifications are related to the spatial scales.

Some authors reported that a room temperature of 27°C significantly influences PORH on the finger pad (peak cutaneous vascular conductance was increased), but the effect was greater on baseline flux (Roustit et al. (2010b)). The same authors reported that lowered room temperature (21°C) tended to decrease PORH baseline and peak cutaneous vascular conductance. However, the authors reported no significant difference compared to the 24°C recordings (Roustit et al. (2010b)). PORH is the sudden increase in cutaneous or muscle blood flow after the release of an arterial occlusion (Mahé et al. (2012)). PORH in the skin is due to several mediators, including sensory nerves and endothelium-derived hyperpolarizing factors. It has recently been shown that prostanoids are not involved in cutaneous PORH in healthy humans (Hellmann et al. (2015)). We now have to study which physiological phenomena come into account to explain the differences we observed between spatial scales.

5. CONCLUSION

Through a recent image processing algorithm dealing with multi-dimensional data (MCEEMDAN algorithm),

we studied the influence of the room temperature on microvascular blood flow recorded with the LSCI modality. Our work reveals that the patterns extracted by MCEEMDAN are influenced by the physiological state (rest, BZ, PORH) and also by the room temperature, specially at PORH. MCEEMDAN could therefore reflect the microvessels state (vasoconstricted or vasodilated state). Furthermore, the influence of the room temperature is different for IMFs and residue. The role played by the room temperature on microvascular blood flow therefore varies with the spatial scales extracted by MCEEMDAN. Our software demonstrator confirms the importance to control the room temperature while performing microvascular investigations. It also brings new research directions to improve the knowledge of temperature regulation of microvascular flow.

REFERENCES

P. Abraham, M. Bourgeau, M. Camo, A. Humeau-Heurtier, S. Durand, P. Rousseau, and G. Mahe. Effect of skin temperature on skin endothelial function assessment. *Microvasc Res.*, 88:56–60, 2013.

M.Z. Ansari, A. Humeau-Heurtier, N. Offenhauser, J.P. Dreier, and A.K. Nirala. Visualization of perfusion changes with laser speckle contrast imaging using the method of motion history image. *Microvasc. Res.*, 107: 106-9, 2016.

D.A. Boas and A.K. Dunn. Laser speckle contrast imaging in biomedical optics. *J. Biomed. Opt.*, 15:011109, 2010. doi: 10.1117/1.3285504.

D. Briers, D.D. Duncan, E. Hirst, S.J. Kirkpatrick, M. Larsson, W. Steenbergen, T. Stromberg, and O.B. Thompson. Laser speckle contrast imaging: theoretical and practical limitations. *J Biomed Opt.*, 18:066018, 2013. doi: 10.1117/1.JBO.18.6.066018.

J.D. Briers and S. Webster. Laser speckle contrast analysis (LASCA): a nonscanning, full-field technique for monitoring capillary blood flow. *J Biomed Opt.*, 1:174-179, 1996.

N. Charkoudian. Skin blood flow in adult human thermoregulation: how it works, when it does not, and why. *Mayo Clin Proc.*, 78:603-612, 2003.

M.A. Colominas, G. Schlotthauer, and M.E. Torres. Improved complete ensemble EMD: A suitable tool for biomedical signal processing. *Biomed. Signal Process. Control*, 14:19-29, 2014.

M. Hellmann, F. Gaillard-Bigot, M. Roustit, and J.L. Cracowski. Prostanoids are not involved in postocclusive reactive hyperaemia in human skin. *Fundam Clin Pharmacol.*, 29:510-6, 2015.

A. Humeau, W. Steenbergen, H. Nilsson, and T. Stromberg. Laser Doppler perfusion monitoring and imaging: novel approaches. *Med Biol Eng Comput.*, 45: 421-35, 2007.

A. Humeau-Heurtier, P. Abraham, S. Durand, and G. Mahé. Excellent inter- and intra-observer reproducibility of microvascular tests using laser speckle contrast imaging. *Clin Hemorheol Microcirc.*, 58:439-46, 2014.

A. Humeau-Heurtier, E. Guerreschi, P. Abraham, and G. Mahé. Relevance of laser Doppler and laser speckle techniques for assessing vascular function: state of the art and future trends. *IEEE Trans Biomed Eng.*, 60: 659-66, 2013.

A. Humeau-Heurtier, G. Mahé, and P. Abraham. Microvascular blood flow monitoring with laser speckle contrast imaging using the generalized differences algorithm. *Microvasc Res.*, 98:54-61, 2015a.

A. Humeau-Heurtier, G. Mahé, and P. Abraham. Multidimensional complete ensemble empirical mode decomposition with adaptive noise applied to laser speckle contrast images. *IEEE Trans Med Imaging*, 34:2103-2117, 2015b.

G. Mahé, A. Humeau-Heurtier, S. Durand, G. Leftheriotis, and P. Abraham. Assessment of skin microvascular function and dysfunction with laser speckle contrast imaging. *Circ Cardiovasc Imaging.*, 5:155-63, 2012.

G.E. Nilsson. Signal processor for laser Doppler tissue flowmeters. *Med Biol Eng Comput.*, 22:343-8, 1984.

G.E. Nilsson, T. Tenland, and P.A. Oberg. A new instrument for continuous measurement of tissue blood flow by light beating spectroscopy. *IEEE Trans Biomed Eng.*, 27:12-9, 1980a.

G.E. Nilsson, T. Tenland, and P.A. Oberg. Evaluation of a laser Doppler flowmeter for measurement of tissue blood flow. *IEEE Trans Biomed Eng.*, 27:597-604, 1980b.

C. Puissant, P. Abraham, S. Durand, A. Humeau-Heurtier, S. Faure, G. Lefthériotis, P. Rousseau, and G. Mahé. Reproducibility of non-invasive assessment of skin endothelial function using laser Doppler flowmetry and laser speckle contrast imaging. *PLoS One*, 8:e61320, 2013.

M. Petrou and P.G. Sevilla. Image processing: dealing with texture. New York, Wiley, 2006.

L.M. Richards, S.M. Kazmi, J.L. Davis, K.E. Olin, and A.K. Dunn. Low-cost laser speckle contrast imaging of blood flow using a webcam. *Biomed Opt Express*, 4: 2269-83, 2013.

P. Rousseau, G. Mahé, F. Haj-Yassin, S. Durand, A. Humeau, G. Leftheriotis, and P. Abraham. Increasing the "region of interest" and "time of interest", both reduce the variability of blood flow measurements using laser speckle contrast imaging. *Microvasc Res.*, 82:88-91, 2011.

M. Roustit, S. Blaise, C. Millet, and J.L. Cracowski. Reproducibility and methodological issues of skin postocclusive and thermal hyperemia assessed by single-point laser Doppler flowmetry. *Microvasc Res.*, 79:102-8, 2010b.

M. Roustit, C. Millet, S. Blaise, B. Dufournet, and J.L. Cracowski. Excellent reproducibility of laser speckle contrast imaging to assess skin microvascular reactivity. *Microvasc Res.*, 80:505-11, 2010a.